

## **Pulmonary Vascular Dilatation Detected by Automated Transcranial Doppler in COVID-19 Pneumonia**

Alexandra S. Reynolds, MD<sup>1</sup>, Alison G. Lee, MD, MS<sup>2</sup>, Joshua Renz, RVT<sup>3</sup>, Katherine DeSantis, MS<sup>3</sup>, John Liang, MD<sup>1</sup>, Charles A. Powell, MD<sup>2</sup>, Corey E. Ventetuolo, MD, MS<sup>4</sup> and Hooman D. Poor, MD<sup>2</sup>

### **Authors' affiliations:**

<sup>1</sup>Departments of Neurosurgery and Neurology, Icahn School of Medicine at Mount Sinai, NY, NY

<sup>2</sup>Division of Pulmonary, Critical Care, and Sleep Medicine, Icahn School of Medicine at Mount Sinai, NY, NY

<sup>3</sup>NovaSignal Corp., Los Angeles, CA

<sup>4</sup>Department of Medicine and Health Services, Policy and Practice, Brown University, Providence, RI

### **Correspondence and request for reprints:**

Hooman D. Poor, MD

Division of Pulmonary, Critical Care, and Sleep Medicine

Icahn School of Medicine at Mount Sinai, NY, NY

10 E. 102<sup>nd</sup> St

New York, NY 10029

Email: [hooman.poor@mountsinai.org](mailto:hooman.poor@mountsinai.org)

Ph: 212-241-5656

Fax: 212-241-8866

**Author's contributions:**

A.S.R.: concept, data gathering, interpretation, drafting of the manuscript

A.G.L.: data analysis, interpretation, drafting of the manuscript

J.R.: data gathering, interpretation, revision of the manuscript

K.D.: data gathering, interpretation, revision of the manuscript

J.L.: concept, revision of the manuscript

C.A.P.: interpretation, revision of the manuscript

C.E.V.: interpretation, data analysis, revision of the manuscript

H.D.P.: concept, data gathering, interpretation, drafting of the manuscript

**Sources of support:**

C.E.V.: R01 HL141268

A.G.L.: K23 HL135349 and R01 MD013310

**Short title:** Pulmonary vasodilatation in COVID-19

**Subject category:** Critical Care 4.2 ALI/ARDS: Diagnosis and Clinical Issues

**Word Count:** 798 words

This article is open access and distributed under the terms of the Creative Commons

Attribution Non-Commercial No Derivatives License 4.0

(<http://creativecommons.org/licenses/by-nc-nd/4.0/>). For commercial usage and reprints

please contact Diane Gern ([dgern@thoracic.org](mailto:dgern@thoracic.org)).

**To the Editor:**

Some patients with COVID-19 pneumonia demonstrate severe hypoxemia despite having near normal lung compliance, a combination not commonly seen in typical acute respiratory distress syndrome (ARDS).<sup>1</sup> The disconnect between gas exchange and lung mechanics in COVID-19 pneumonia has raised the question of whether the mechanisms of hypoxemia in COVID-19 pneumonia differ from those in classical ARDS. Dual-energy CT imaging has demonstrated pulmonary vessel dilatation<sup>2</sup> and autopsies have shown pulmonary capillary deformation<sup>3</sup> in patients with COVID-19 pneumonia.

Contrast enhanced transcranial Doppler (TCD) of the bilateral middle cerebral arteries following injection of agitated saline is an ultrasound technique, similar to transthoracic or transesophageal echocardiography, that can be performed to detect microbubbles and diagnose intracardiac or intrapulmonary shunt (Figure 1).<sup>4,5</sup> TCD is more sensitive than transthoracic echocardiography in detecting right to left shunt,<sup>6</sup> and is less invasive than transesophageal echocardiography. We performed a cross-sectional pilot study of TCD (Lucid Robotic System, NovaSignal Corp., Los Angeles CA USA) in all mechanically ventilated patients with severe COVID-19 pneumonia from two COVID-19 intensive care units who were not undergoing continuous renal replacement therapy or extracorporeal membrane oxygenation (N=18). This study was approved by the Mount Sinai Institutional Review Board (IRB approval 20-03660). Agitated saline was injected through either a peripheral IV in the upper extremity or a central line in the internal jugular vein. The system software automatically counted the number of microbubbles detected over 20 seconds; as a quality control measure, we manually counted and confirmed the number of microbubbles and were blinded to the patients'

clinical condition and PaO<sub>2</sub>:FiO<sub>2</sub> ratio. Sixty-one percent (N=11) of patients were men. Patients had a median age of 59 years (interquartile range 54 to 68) with a PaO<sub>2</sub>:FiO<sub>2</sub> ratio of 127 mmHg (interquartile range 94 to 173). Lung compliance was measured in 16 patients and was low (median 22 mL/cmH<sub>2</sub>O, interquartile range 15 to 34). None of the patients had a known history of chronic liver disease or pre-existing intracardiac shunt. Contrast-enhanced TCD detected a median of 8 microbubbles (interquartile range 1 to 22, range 0 to 300). Three major findings from contrast-enhanced TCD were observed. First, 15/18 (83%) of patients had detectable microbubbles (see Figure 1 for representative images). Second, the PaO<sub>2</sub>:FiO<sub>2</sub> ratio was inversely correlated with the number of microbubbles (Pearson's  $r = -0.55$ ,  $p = 0.02$ , Figure 2A). Third, the number of microbubbles was inversely correlated to lung compliance (Pearson's  $r = -0.61$ ,  $p = 0.01$ , Figure 2B).

These data suggest that pulmonary vasodilatations may explain the disproportionate hypoxemia in some patients with COVID-19 pneumonia and, somewhat surprisingly, track with poor lung compliance.<sup>1</sup> Our detection of transpulmonary bubbles may be analogous to hepatopulmonary syndrome (HPS), a pulmonary vascular disorder of chronic liver disease characterized by pulmonary vascular dilatations with increased blood flow to affected lung units, which results in ventilation-perfusion mismatch and hypoxemia.<sup>4</sup> The normal lung filters microbubbles from the injection of agitated saline as the bubble diameter is larger (smallest bubble approximately 24  $\mu\text{m}$  in diameter<sup>5</sup>) than the normal pulmonary capillary (<15  $\mu\text{m}$  in diameter<sup>7</sup>). In HPS, and similar to what we observed in this pilot study, the presence and degree of transpulmonary bubble transit correlate with the degree of hypoxemia.<sup>8</sup>

While we cannot rule out intracardiac shunt as a cause of observed microbubbles, we note that the prevalence of transpulmonary bubbles seen in our study is markedly higher than the prevalence of patent foramen ovale seen in the general population.<sup>9</sup> In a prior study of 265 patients with ARDS receiving mechanical ventilation, only 42 patients (16%) were found to have patent foramen ovale as assessed by contrast transesophageal echocardiography.<sup>10</sup>

Hypoxemia in ARDS is predominantly caused by right-to-left shunt, where systemic venous blood flows to lung regions with collapsed and/or flooded alveoli and does not get oxygenated as it passes through the lung.<sup>11</sup> Transpulmonary bubble transit has been detected in 26% of patients with classical ARDS, though neither their presence nor their severity correlates with oxygenation<sup>10</sup>, implying that pulmonary vascular dilatations are not a major mechanism of hypoxemia in typical ARDS. In order for transpulmonary bubble transit to occur, pulmonary vascular dilatations or pulmonary arteriovenous malformations must be present; a lack of hypoxic vasoconstriction is not sufficient. While these observations are preliminary, the correlation seen here between the degree of transpulmonary bubble transit and  $\text{PaO}_2:\text{FiO}_2$  ratio suggests that pulmonary vascular dilatation may be a significant cause of hypoxemia in patients with COVID-19 respiratory failure. Interestingly, patients with worse lung compliance demonstrated more microbubbles, which suggests that pulmonary vascular dilatation may worsen in parallel with the typical diffuse alveolar damage of ARDS.

Our understanding of the pathophysiology of hypoxemic respiratory in COVID-19 is limited. While a larger, confirmatory study is needed, these data, in conjunction with

recent radiographic and autopsy findings, seem to implicate pulmonary vascular dilatation as a cause of hypoxemia in patients with COVID-19 pneumonia.

## References:

1. Gattinoni, L, Coppola S, Cressoni M, et al. Covid-19 does not lead to “typical” Acute Respiratory Distress Syndrome. *Am J Respir Crit Care Med*. 2020 Mar 30.
2. Lang M, Som A, Mendoza D, et al. Hypoxaemia related to COVID-19: vascular and perfusion abnormalities on dual-energy CT. *Lancet Infect Dis*. 2020 Apr 30
3. Ackerman M, Verleden S, Kuehnel M, et al. Pulmonary Vascular Endothelialitis, Thrombosis, and Angiogenesis in Covid-19. *N Engl J Med*. 2020 May 21
4. Ramirez Moreno JM, Millan Nunez MV, Rodriguez Carrasco M, et al. Detection of an intrapulmonary shunt in patients with liver cirrhosis through contrast-enhanced transcranial Doppler. A study of prevalence, pattern characterization and diagnostic validity. *Gastroenterol Hepatol*. 2015 38:475-83.
5. Teague S, Sharma M. Detection of paradoxical cerebral echo contrast embolization by transcranial Doppler ultrasound. *Stroke*. 1991 22:740-5.
6. Katsanos A, Psaltopoulou T, Sergetanis T, et al. Transcranial Doppler versus transthoracic echocardiography for the detection of patent foramen ovale in patients with cryptogenic cerebral ischemia: A systematic review and diagnostic test accuracy meta-analysis. *Ann Neurol*. 2016 79:625-35.
7. Townsley M. Structure and composition of pulmonary arteries, capillaries and veins. *Compr Physiol*. 2012 Jan 2:675-709.

8. Fischer C, Campos O, Fernandes W, et al. Role of contrast-enhanced transesophageal echocardiography for detection of and scoring intrapulmonary vascular dilatation. *Echocardiography* 2010 27:1233-7.
9. Hagen PT, Scholz DG, Edwards WD. Incidence and size of patent foramen ovale during the first 10 decades of life: an autopsy study of 965 normal hearts. *Mayo Clin Proc* 1984;59(1):17-20.
10. Boissier F, Razazi K, Thille A, et al. Echocardiographic detection of transpulmonary bubble transit during acute respiratory distress syndrome. *Ann Intensive Care*. 2015 205; 5: 5.
11. Dantzker D, Brook C, Dehart P, et al. Ventilation-perfusion distributions in the adult respiratory distress syndrome. *Am Rev Respir Dis*. 1979 120:1039-52.



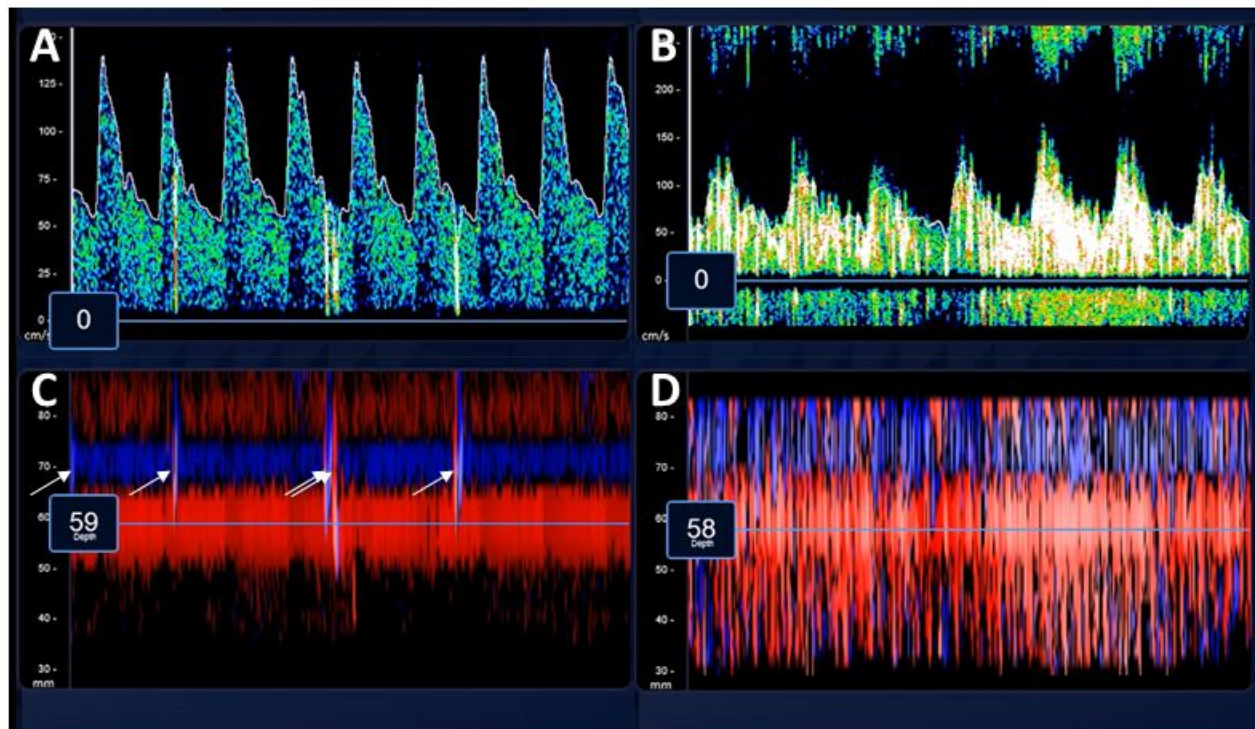
**Figure Legends:****1. Assessment of microbubbles by transcranial Doppler following injection of agitated saline.**

Representative images captured during transcranial Doppler (TCD) evaluation after injection of agitated saline. Panels A and B demonstrate the continuous spectral waveforms of the middle cerebral artery (MCA) during insonation over 5 seconds. Panels C and D demonstrate the power M-mode, and positive microbubbles appear as vertical lines (arrows). Panels A and C are images from the left MCA of a 60-year-old woman where TCD detected five microbubbles. Panels B and D are images from the right MCA of a 69-year-old man where TCD detected 300 microbubbles. His  $\text{PaO}_2:\text{FiO}_2$  ratio was 55 mmHg, which was the lowest in the cohort.

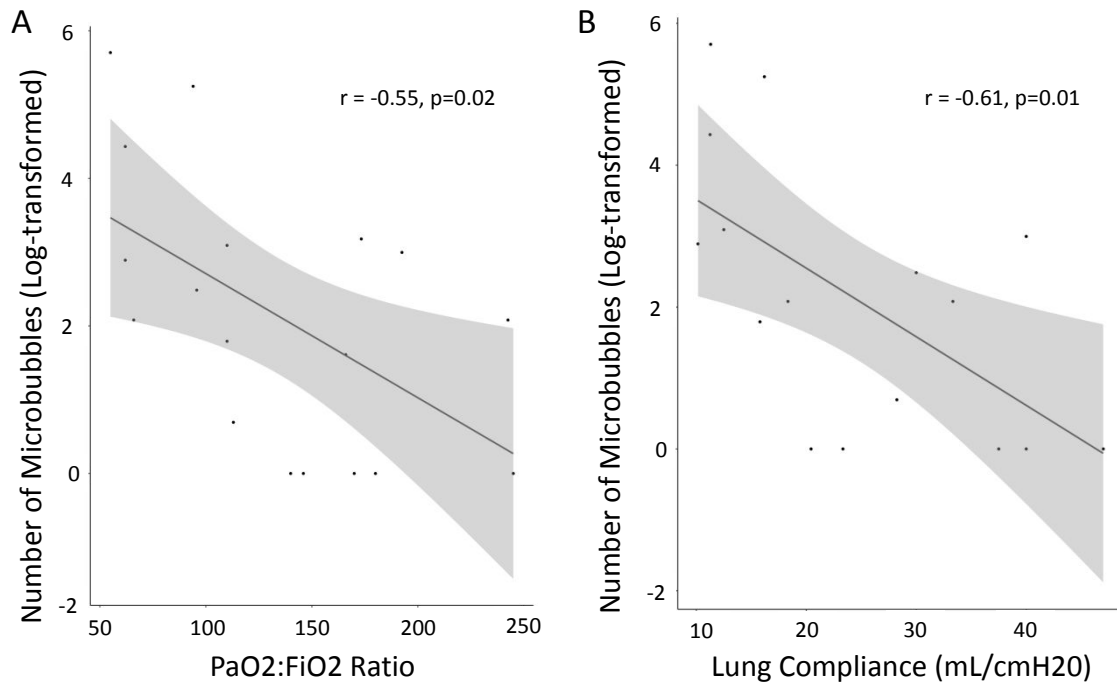
**2. Associations between number of microbubbles and  $\text{PaO}_2:\text{FiO}_2$  ratio and lung compliance.**

Panel A represents a scatterplot of log-transformed number of microbubbles as detected by transcranial Doppler and  $\text{PaO}_2:\text{FiO}_2$  ratio ( $r = -0.55$ ,  $p = 0.02$ ) and suggests that the number of microbubbles increases with declining  $\text{PaO}_2:\text{FiO}_2$  ratio. Panel B represents a scatterplot of log-transformed number of microbubbles as detected by transcranial Doppler and lung compliance ( $r = -0.61$ ,  $p = 0.01$ ) and suggests that the number of microbubbles increases with declining lung compliance.

Figure 1



**Figure 1. Assessment of microbubbles by transcranial Doppler following injection of agitated saline.** Representative images captured during transcranial Doppler (TCD) evaluation after injection of agitated saline. Panels A and B demonstrate the continuous spectral waveforms of the middle cerebral artery (MCA) during insonation over 5 seconds. Panels C and D demonstrate the power M-mode, and positive microbubbles appear as vertical lines (arrows). Panels A and C are images from the left MCA of a 60-year-old woman where TCD detected five microbubbles. Panels B and D are images from the right MCA of a 69-year-old man where TCD detected 300 microbubbles. His PaO<sub>2</sub>:FiO<sub>2</sub> ratio was 55 mmHg, which was the lowest in the cohort.

**Figure 2**

**Figure 2. Associations between number of microbubbles and PaO<sub>2</sub>:FiO<sub>2</sub> ratio and lung compliance** Panel A represents a scatterplot of log-transformed number of microbubbles as detected by transcranial Doppler and PaO<sub>2</sub>:FiO<sub>2</sub> ratio ( $r = -0.55$ ,  $p = 0.02$ ) and suggests that the number of microbubbles increases with declining PaO<sub>2</sub>:FiO<sub>2</sub> ratio. Panel B represents a scatterplot of log-transformed number of microbubbles as detected by transcranial Doppler and lung compliance ( $r = -0.61$ ,  $p = 0.01$ ) and suggests that the number of microbubbles increases with declining lung compliance.